

$\mathbf{H}(\text{curl})$ auxiliary mesh preconditioning[†]

Tzanio V. Kolev¹, Joseph E. Pasciak² and Panayot S. Vassilevski^{1,*,†}

¹*Center for Applied Scientific Computing, UC Lawrence Livermore National Laboratory, P.O. Box 808, L-560, Livermore, CA 94551, U.S.A.*

²*Department of Mathematics, Texas A & M University, College Station, TX 77843-3368, U.S.A.*

SUMMARY

This paper analyses a two-level preconditioning scheme for $\mathbf{H}(\text{curl})$ bilinear forms. The scheme utilizes an auxiliary problem on a related mesh that is more amenable for constructing optimal order multigrid methods. More specifically, we analyse the case when the auxiliary mesh only approximately covers the original domain. The latter assumption is important since it allows for easy construction of nested multilevel spaces on regular auxiliary meshes. Numerical experiments in both two and three space dimensions illustrate the optimal performance of the method. Published in 2007 by John Wiley & Sons, Ltd.

Received 8 January 2007; Accepted 10 January 2007

KEY WORDS: auxiliary mesh preconditioning; $\mathbf{H}(\text{curl})$ problems; Nédélec spaces

1. INTRODUCTION

This paper analyses a two-level preconditioning scheme for the $\mathbf{H}(\text{curl})$ problem previously developed for elliptic finite-element problems (cf. [1–3]). A main motivation for such an approach is to be able to solve finite-element problems posed on unstructured meshes by methods available for discretizations of the same partial differential equation on a related auxiliary mesh for which preconditioners (for example of multigrid type) are easier to construct. The two-level auxiliary mesh scheme, in combination with a related domain embedding technique (or ‘fictitious’ domain methods, going back as early as to [4, 5]) may be seen as a more practical motivation for the kind of study we have taken in the present paper. The specific problem we consider comes

*Correspondence to: Panayot S. Vassilevski, Center for Applied Scientific Computing, UC Lawrence Livermore National Laboratory, P.O. Box 808, L-560, Livermore, CA 94551, U.S.A.

†E-mail: panayot@llnl.gov

‡This article is a U.S. Government work and is in the public domain in the U.S.A.

Contract/grant sponsor: U.S. Department of Energy by the University of California Lawrence Livermore National Laboratory; contract/grant number: W-7405-Eng-48

from Maxwell equations and leads to a bilinear form on the space $\mathbf{H}(\Omega; \text{curl})$ for a 3D polyhedral domain Ω . For simplicity, we take Ω to be simply connected with a connected boundary. Since the resulting form is not equivalent to a standard second order elliptic one, the analysis we present is a bit more involved, a main part of which is to establish that a discrete de Rham diagram commutes for two sequences of non-related finite-element spaces and the natural interpolation operators associated with them.

Our result is closely related to those of a recent paper [6] dealing with the same topic. The difference is that our analysis is more general; in particular, it applies to the lowest order Nédélec space whereas the result in [6] substantially relies on the fact that the auxiliary Nédélec space contains an \mathbf{H}^1 -conforming subspace. Another difference is that we provide experiments in three dimensions. A main ingredient in the implementation is the construction of the mapping $\mathbf{\Pi}_h^Q$ that relates the auxiliary mesh Nédélec space \mathbf{Q}_H with the original one \mathbf{Q}_h (for more details see Section 3). As it turned out, the newly proposed multilevel method by Hiptmair and Xu [7] utilizes a similar operator that, however, relates a \mathbf{H}^1 -conforming space \mathbf{S}_h on the same mesh with the original Nédélec space \mathbf{Q}_h . That is, the method in [7] does not require remeshing the domain; it uses a \mathbf{H}^1 -conforming auxiliary space on the original mesh, instead. Our present implementation of $\mathbf{\Pi}_h^Q$ is somewhat involved since it is computed as a mapping from a finite-element space defined on a different (auxiliary) mesh into a space on the original mesh. However, it enabled us to easily implement and test the performance, both in serial and in parallel (see [8, 9]) of a modified version of the method in [7]. Combining both approaches (from the present paper and [7]) we can allow auxiliary meshes that do not completely cover the original domain and either use auxiliary Nédélec spaces or auxiliary \mathbf{H}^1 -conforming spaces on them to construct efficient auxiliary mesh/space preconditioners.

The remainder of the paper is structured as follows. In Section 2 we pose the problem, define the two-level preconditioning scheme in general terms, and give details about the auxiliary mesh and space. In Section 3 the main properties of the mapping $\mathbf{\Pi}_h^Q$ are stated. Then, in Section 4 the so-called Hiptmair smoother is reviewed. Section 5 contains the proof of our main theorem. The commuting property of the discrete de Rham diagram and a related L^2 -stability of the natural interpolation operators associated with it are the main subject of Section 6. Finally, numerical experiments both in two and three space dimensions illustrating the theory are presented in Section 7.

2. THE $\mathbf{H}(\text{curl})$ PROBLEM AND ITS TWO-LEVEL PRECONDITIONING

We shall denote $\mathbf{L}^2(\Omega)$ to be the space of vector functions on Ω whose components are in $L^2(\Omega)$. For scalar and vector functions, we shall use (\cdot, \cdot) to denote the inner product both in $\mathbf{L}^2(\Omega)$ and $L^2(\Omega)$. The corresponding norm will be denoted $\|\cdot\|_0$ while the norm on $H^1(\Omega)$ and $\mathbf{H}^1(\Omega) \equiv H^1(\Omega)^3$ will be denoted $\|\cdot\|_1$.

We consider the following bilinear form

$$A(\mathbf{u}, \mathbf{v}) = (\mathbf{u}, \mathbf{v}) + (\nabla \times \mathbf{u}, \nabla \times \mathbf{v})$$

for functions \mathbf{u}, \mathbf{v} in $\mathbf{H}(\Omega; \text{curl}) \equiv \{\mathbf{u} \in \mathbf{L}^2(\Omega) : \nabla \times \mathbf{u} \in \mathbf{L}^2(\Omega)\}$. We also consider the subspace $\mathbf{H}_0(\Omega; \text{curl})$ of functions \mathbf{u} in $\mathbf{H}(\Omega; \text{curl})$ which satisfy homogeneous Dirichlet boundary conditions, i.e. $\mathbf{u} \times \mathbf{n} = 0$ on $\partial\Omega$. Similarly, $\mathbf{H}_0(\Omega; \text{div})$ stands for the space of functions $\mathbf{u} \in \mathbf{H}(\Omega; \text{div}) \equiv \{\mathbf{u} \in \mathbf{L}^2(\Omega) : \nabla \cdot \mathbf{u} \in L^2(\Omega)\}$ satisfying $\mathbf{u} \cdot \mathbf{n} = 0$ on $\partial\Omega$.

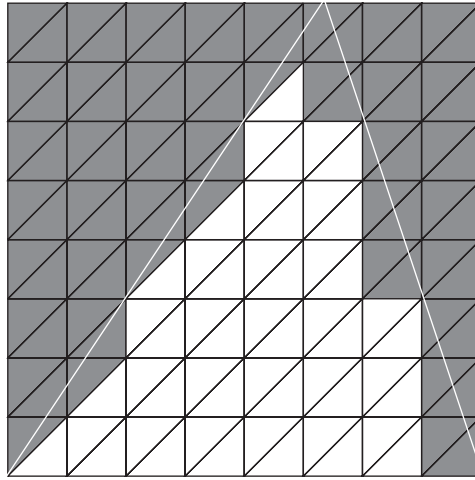


Figure 1. Example of an auxiliary mesh \mathcal{T}_H (in white) embedded in the original triangular domain Ω .

We assume that Ω is triangulated by a quasi-uniform mesh \mathcal{T}_h consisting of tetrahedrons of size h . Let P_r be the space of polynomials of degree at most r and \mathbf{P}_r denote P_r^3 . We associate with \mathcal{T}_h the $\mathbf{H}_0(\Omega; \text{curl})$ -conforming Nédélec space \mathbf{Q}_h of order r . On each element $K \in \mathcal{T}_h$, functions in \mathbf{Q}_h are polynomials of degree at most $r + 1$ of the form

$$\mathbf{P}(\mathbf{x}) = \mathbf{Q}(\mathbf{x}) + \mathbf{R}(\mathbf{x})$$

where $\mathbf{Q} \in \mathbf{P}_r$ and \mathbf{R} is a homogeneous vector polynomial of degree $r + 1$ satisfying $\mathbf{R} \cdot \mathbf{x} = 0$ for all $\mathbf{x} \in \mathbb{R}^3$.

The form $A(\cdot, \cdot)$ restricted to $\mathbf{Q}_h \times \mathbf{Q}_h$ defines a symmetric and positive-definite operator A_h , i.e. for $\mathbf{v} \in \mathbf{Q}_h$, $A_h \mathbf{v}$ is the unique function in \mathbf{Q}_h satisfying

$$(A_h \mathbf{v}, \boldsymbol{\theta}) = A(\mathbf{v}, \boldsymbol{\theta}) \quad \text{for all } \boldsymbol{\theta} \in \mathbf{Q}_h \tag{1}$$

Our goal in this paper is to construct a two-level preconditioner B_h for A_h which utilizes an auxiliary mesh \mathcal{T}_H obtained by using a mesh whose elements consist of the elements of a uniform mesh which are contained in Ω (see Figure 1). Such a mesh does not fit the domain Ω but is a reasonable approximation to it. Multilevel algorithms are easy to set up for this mesh if we take the original H -mesh to be a geometrically refined uniform grid. Let \mathbf{Q}_H denote the Nédélec space associated with the mesh \mathcal{T}_H of functions in $\mathbf{H}_0(\Omega_H; \text{curl})$ where $\Omega_H = \bigcup T$, $T \in \mathcal{T}_H$, and $T \subset \Omega$. By extension by zero, we can consider functions in \mathbf{Q}_H as a subset of $\mathbf{H}_0(\Omega; \text{curl})$.

We assume that the meshes \mathcal{T}_h and \mathcal{T}_H are roughly of the same size, i.e. $C_0 h \leq H \leq C_1 h$ and denote that with $h \simeq H$. Here and in the remainder of this paper, C , with or without subscript, denotes a generic positive constant which is independent of h .

The resulting preconditioner B_h involves smoothing on \mathbf{Q}_h and an auxiliary preconditioner B_H for the problem on \mathbf{Q}_H (see Remark 5.1). Specifically, the two-level operator B_h , is defined by

$$B_h = R_h + \Pi_h^{\mathbf{Q}} B_H (\Pi_h^{\mathbf{Q}})^T \tag{2}$$

where R_h is the smoothing operator on \mathbf{Q}_h and B_H denotes a multilevel preconditioner on \mathbf{Q}_H . Here $\mathbf{\Pi}_h^Q$ denotes the natural interpolation operator associated with the Nédélec space \mathbf{Q}_h and $(\mathbf{\Pi}_h^Q)^T$ denotes its $L^2(\Omega)$ adjoint. The construction and analysis of geometric multigrid preconditioners B_H for the problem on \mathbf{Q}_H (when the mesh of \mathcal{T}_H fills Ω) has been well researched [10–13]. It results in an operator $B_H : \mathbf{Q}_H \rightarrow \mathbf{Q}_H$ satisfying

$$c_0 A(\mathbf{v}, \mathbf{v}) \leq (B_H^{-1} \mathbf{v}, \mathbf{v}) \leq c_1 A(\mathbf{v}, \mathbf{v}) \quad \text{for all } \mathbf{v} \in \mathbf{Q}_H \tag{3}$$

with constants c_0, c_1 independent of H . We stress the fact that our result holds even when the elements of \mathcal{T}_H do not fill Ω (but approximate it of order $H \simeq h$). Our numerical experiments clearly support these findings.

From (3) and the fact that B_h is an additive algorithm, the analysis of B_h reduces to that of the preconditioner with the exact solve on \mathbf{Q}_H , i.e.

$$\tilde{B}_h = R_h + \mathbf{\Pi}_h^Q A_H^{-1} (\mathbf{\Pi}_h^Q)^T \tag{4}$$

Here A_H is the operator corresponding to $A(\cdot, \cdot)$ on \mathbf{Q}_H (analogous to (1)).

The following well-known identity (cf. e.g. [14, Lemma 1, p. 154]) holds: for $\mathbf{v}_h \in \mathbf{Q}_h$

$$(\tilde{B}_h^{-1} \mathbf{v}_h, \mathbf{v}_h) = \inf_{\mathbf{v}_h = \mathbf{w}_h + \mathbf{\Pi}_h^Q \mathbf{v}_H} \{ (R_h^{-1} \mathbf{w}_h, \mathbf{w}_h) + A_H(\mathbf{v}_H, \mathbf{v}_H) \} \tag{5}$$

The infimum is taken over all decompositions of the above form with $\mathbf{w}_h \in \mathbf{Q}_h$ and $\mathbf{v}_H \in \mathbf{Q}_H$.

3. THE ANALYSIS OF $\mathbf{\Pi}_h^Q$

In this section, we derive some properties of $\mathbf{\Pi}_h^Q$, specifically, we need to check how it behaves when applied to functions in \mathbf{Q}_H . Actually, we shall have to deal with all of the corresponding operators which appear in the de Rham sequence. Specifically, we denote by S_h the functions in $H_0^1(\Omega)$ whose restriction to $K \in \mathcal{T}_h$ are in P_r . We also denote the Raviart–Thomas space \mathbf{R}_h to be the set of functions in $\mathbf{H}_0(\Omega; \text{div})$ whose restriction to $K \in \mathcal{T}_h$ are polynomials of the form

$$\mathbf{P}(\mathbf{x}) = \mathbf{Q}(\mathbf{x}) + R(\mathbf{x})\mathbf{x}$$

where $\mathbf{Q} \in \mathbf{P}_r$ and R is a homogeneous polynomial of degree r . We then have the exact sequence

$$0 \longrightarrow S_h \xrightarrow{\nabla} \mathbf{Q}_h \xrightarrow{\nabla \times} \mathbf{R}_h$$

The analogous spaces on the mesh \mathcal{T}_H are denoted S_H, \mathbf{Q}_H and \mathbf{R}_H . These have zero nodal components on the boundary of Ω_H and are extended by zero to Ω .

Along with the spaces S_h, \mathbf{Q}_h and \mathbf{R}_h , there are natural interpolation operators (see, e.g. [15, 16]) $\mathbf{\Pi}_h^S, \mathbf{\Pi}_h^Q$ and $\mathbf{\Pi}_h^R$. These operators are defined for sufficiently smooth functions, e.g. $\mathbf{\Pi}_h^S$ is defined on functions in $H^{1+s}(\Omega)$ for any $s > 0$. $\mathbf{\Pi}_h^Q$ is defined for functions $\mathbf{v} \in \mathbf{H}^s(\Omega)$ for $s > \frac{1}{2}$ satisfying $\nabla \times \mathbf{v} \in \mathbf{L}^p(\Omega)$ for $p > 2$ [17]. Finally, $\mathbf{\Pi}_h^R$ is defined for functions $\mathbf{v} \in \mathbf{H}^s(\Omega)$ with $s > 0$ satisfying $\nabla \cdot \mathbf{v} \in L^p(\Omega)$ for $p > 2$.

From the above discussion, it is not clear that the interpolation operator Π_h^Q is even well defined on \mathbf{Q}_H . That this is the case is given by the following theorem whose proof appears later.

Theorem 3.1

The interpolation operators Π_h^S , Π_h^Q and Π_h^R are well defined on S_H , \mathbf{Q}_H and \mathbf{R}_H . Furthermore, they are stable, respectively, in the $L^2(\Omega)$ and $\mathbf{L}^2(\Omega)$ norms on these spaces and the following diagram commutes:

$$\begin{array}{ccccc}
 S_H & \xrightarrow{\nabla} & \mathbf{Q}_H & \xrightarrow{\nabla \times} & \mathbf{R}_H \\
 \Pi_h^S \downarrow & & \Pi_h^Q \downarrow & & \Pi_h^R \downarrow \\
 S_h & \xrightarrow{\nabla} & \mathbf{Q}_h & \xrightarrow{\nabla \times} & \mathbf{R}_h
 \end{array} \tag{6}$$

As a consequence one gets the following stability result:

Corollary 3.1

For $\mathbf{u} \in \mathbf{Q}_H$,

$$\|\nabla \times \Pi_h^Q \mathbf{u}\|_0 = \|\Pi_h^R(\nabla \times \mathbf{u})\|_0 \leq C \|\nabla \times \mathbf{u}\|_0$$

that is, Π_h^Q is stable in the $\mathbf{H}(\Omega; \text{curl})$ -norm on \mathbf{Q}_H .

Remark 3.1

The proof of the above theorem actually shows that

$$\|\Pi_h^Q \mathbf{w}_H\|_{0,K} \leq C \|\mathbf{w}_H\|_{0,\hat{K}} \quad \text{for all } \mathbf{w}_H \in \mathbf{Q}_H$$

and

$$\|\Pi_h^S v_H\|_{0,K} \leq C \|v_H\|_{0,\hat{K}} \quad \text{for all } v_H \in S_H$$

Here K is a given element from \mathcal{T}_h and \hat{K} is a union of \mathcal{T}_H elements that intersect K .

Let v_H be in S_H . Set \bar{v}_H be the mean value of v_H on \hat{K} if $\hat{K} \cap \partial\Omega = \emptyset$, otherwise, set $\bar{v}_H = 0$. We note that

$$\|v_H - \bar{v}_H\|_{0,\hat{K}} \leq Ch \|v_H\|_{1,\hat{K}} \tag{7}$$

Such inequalities for clusters \hat{K} which are star shaped with respect to a ball are given in [18]. A more general argument is given in [1]. We then have

$$\|v_H - \Pi_h^S v_H\|_{0,K} \leq C \|v_H - \bar{v}_H\|_{0,K} + \|\Pi_h^S(v_H - \bar{v}_H)\|_{0,K} \leq Ch \|v_H\|_{1,\hat{K}}$$

where we used the above remark and (7) for the last inequality. The inequality

$$\|v_H - \Pi_h^S v_H\|_0 \leq Ch \|v_H\|_1$$

follows by summation. Finally, using the Clement operator \tilde{Q}_h , which satisfies

$$\|v - \tilde{Q}_h v\|_0 + h \|\tilde{Q}_h v\|_1 \leq Ch \|v\|_1 \quad \text{for any } v \in H^1(\Omega)$$

and the triangle and inverse inequalities, we get

$$\begin{aligned} \|\Pi_h^S v\|_1 &\leq \|\tilde{Q}_h v - \Pi_h^S v\|_1 + \|\tilde{Q}_h v\|_1 \\ &\leq Ch^{-1} \|\tilde{Q}_h v - \Pi_h^S v\|_0 + C\|v\|_1 \\ &\leq Ch^{-1} \|\tilde{Q}_h v - v\|_0 + Ch^{-1} \|\Pi_h^S v - v\|_0 + C\|v\|_1 \\ &\leq C\|v\|_1 \end{aligned}$$

That is, we have

$$\|v - \Pi_h^S v\|_0 + h\|\Pi_h^S v\|_1 \leq Ch\|v\|_1 \quad \text{for all } v \in S_H \quad (8)$$

This estimate is non-standard in that it fails to hold for general H^1 functions as the nodal values are not well defined there.

Also, if $\mathbf{z}_h \in \mathbf{S}_h \equiv S_h^3$ then

$$\|\mathbf{z}_h - \Pi_h^Q \mathbf{z}_h\|_0 \leq Ch\|\mathbf{z}_h\|_1 \quad (9)$$

and, for $K \in \mathcal{T}_h$

$$\|\Pi_h^Q \mathbf{z}_h\|_{0,K} \leq C\|\mathbf{z}_h\|_{0,K} \quad (10)$$

The inequality (9) depends on \mathbf{z}_h being piecewise polynomial on the h -mesh while (10) follows from a simple scaling argument. Finally, (9) and an inverse inequality (when applied to H) implies

$$\|\Pi_H^Q \mathbf{z}_H\|_{\mathbf{H}(\Omega; \text{curl})} \leq C\|\mathbf{z}_H\|_1 \quad \text{for all } \mathbf{z}_H \in \mathbf{S}_H \quad (11)$$

4. THE HIPTMAIR SMOOTHER

We can now define the so-called ‘Hiptmair’ smoother. Let $\{\theta_j\}_{j=1}^M$ be a nodal basis for S_h and $\{\phi_k\}_{k=1}^N$ be the nodal basis for \mathbf{Q}_h . We consider the set $\{\Theta_i\} = \{\phi_j\} \cup \{\nabla\theta_j\}$ and define the one-dimensional subspace $\mathbf{Q}_{h,i}$ to be the span of Θ_i , $i = 1, \dots, N + M$. We let $Q_{h,i}$ and $P_{h,i}$, respectively, denote the $L^2(\Omega)$ and $A(\cdot, \cdot)$ projectors onto $\mathbf{Q}_{h,i}$.

The Hiptmair smoother is defined to be the additive smoother associated with these spaces, i.e.

$$R_h = \sum_{i=1}^{N+M} A_{h,i}^{-1} Q_{h,i}$$

Here $A_{h,i} : \mathbf{Q}_{h,i} \rightarrow \mathbf{Q}_{h,i}$ is defined by

$$(A_{h,i} v, w) = A(v, w) \quad \text{for } v, w \in \mathbf{Q}_{h,i}$$

Similar to (5), we have the identity

$$(R_h^{-1} \mathbf{w}_h, \mathbf{w}_h) = \inf \left(\sum_{i=1}^N A(v_i, v_i) + \sum_{i=N+1}^{N+M} (\nabla p_i, \nabla p_i) \right)$$

Here $v_i \in \mathbf{Q}_{h,i}$, $i = 1, \dots, N$, $\nabla p_i \in \mathbf{Q}_{h,i}$, $i = N + 1, \dots, N + M$ and the infimum is taken over all such decompositions of \mathbf{w}_h . It follows from the limited overlap of nodal basis functions that

$$A(\mathbf{w}_h, \mathbf{w}_h) \leq C(R_h^{-1} \mathbf{w}_h, \mathbf{w}_h) \tag{12}$$

Now if $\mathbf{w}_h = \mathbf{v}_h + \nabla p_h$ and we decompose $\mathbf{v}_h = \sum_{i=1}^N v_i$ and $p_h = \sum_{i=N+1}^{N+M} p_i$ then we get

$$(R_h^{-1} \mathbf{w}_h, \mathbf{w}_h) \leq c h^{-2} (\|\mathbf{v}_h\|_0^2 + \|p_h\|_0^2) \tag{13}$$

5. THE MAIN THEOREM

We prove the main theorem estimating the condition number of the preconditioned system corresponding to the proposed two-level method in this section. We start with the following theorem proved in [7]. Its proof was based on the decomposition (cf. [10, 19]) of functions in $\mathbf{H}_0(\Omega; \text{curl})$ into a function in $\mathbf{H}_0^1(\Omega)$ and a gradient of a function in $H_0^1(\Omega)$.

Theorem 5.1

A function $\mathbf{u}_h \in \mathbf{Q}_h$ can be decomposed as

$$\mathbf{u}_h = \mathbf{v}_h + \mathbf{\Pi}_h^Q \mathbf{z}_h + \nabla p_h \tag{14}$$

where $\mathbf{v}_h \in \mathbf{Q}_h$, $\mathbf{z}_h \in \mathbf{S}_h$, $p_h \in S_h$ satisfy

$$h^{-1} \|\mathbf{v}_h\|_0 + \|\mathbf{z}_h\|_1 + \|\nabla p_h\|_0 \leq C \|\mathbf{u}_h\|_{\mathbf{H}(\Omega; \text{curl})}$$

Using the above theorem and earlier results, we get our main result.

Theorem 5.2

There are constants c_1 and c_2 independent of h satisfying

$$c_1 A(\mathbf{u}, \mathbf{u}) \leq A(\tilde{B}_h A_h \mathbf{u}, \mathbf{u}) \leq c_2 A(\mathbf{u}, \mathbf{u}) \quad \text{for all } \mathbf{u} \in \mathbf{Q}_h$$

Proof

The above inequality is equivalent to

$$c_2^{-1} A(\mathbf{u}_h, \mathbf{u}_h) \leq (\tilde{B}_h^{-1} \mathbf{u}_h, \mathbf{u}_h) \leq c_1^{-1} A(\mathbf{u}_h, \mathbf{u}_h) \quad \text{for all } \mathbf{u}_h \in \mathbf{Q}_h \tag{15}$$

For the first inequality, we have

$$A(\mathbf{v}_h, \mathbf{v}_h) \leq 2(A(\mathbf{w}_h, \mathbf{w}_h) + A(\mathbf{\Pi}_h^Q \mathbf{v}_H, \mathbf{\Pi}_h^Q \mathbf{v}_H))$$

where we have decomposed \mathbf{v}_h as in (5). The first inequality in (15) then follows from (12) and Corollary 3.1.

For the other direction, we start from the decomposition (14). We note that one can choose $\mathbf{z}_H \in \mathbf{S}_H$ and $p_H \in S_H$ such that for $H \simeq h$,

$$\begin{aligned} h^{-1} \|\mathbf{z}_h - \mathbf{z}_H\|_0 + \|\mathbf{z}_H\|_1 &\leq C \|\mathbf{z}_h\|_1 \\ h^{-1} \|p_h - p_H\|_0 + \|p_H\|_1 &\leq C \|p_h\|_1 \end{aligned} \tag{16}$$

We illustrate the case of p_H as that of \mathbf{z}_H is identical. Let $\bar{\Omega}_H = \bigcup T$, T in the H -mesh, $T \cap \Omega \neq \emptyset$. Let \tilde{p}_H denote interpolant of p_h (extended by zero outside of Ω) with respect to the extended H -grid on $\bar{\Omega}_H$. We define p_H to be \tilde{p}_H on the interior vertices of Ω_H and set $p_H(v_i) = 0$ on the vertices of $\partial\Omega_H$. Now (8) holds with h and H interchanged (using the extended H -mesh). Thus, by the triangle inequality, (16) will follow if we show that

$$h^{-1} \|\tilde{p}_H - p_H\|_0 + \|\tilde{p}_H - p_H\|_1 \leq C \|\tilde{p}_H\|_{1, \bar{\Omega}_H}$$

Note that $\tilde{p}_H - p_H$ lives on the H -elements which intersect $\partial\Omega_H$ and \tilde{p}_H vanishes on $\partial\bar{\Omega}_H$. Let $\{\varphi_i^{(H)}\}$ be the standard nodal piecewise linear basis functions associated with the extended \mathcal{T}_H mesh. Then

$$\tilde{p}_H - p_H = \sum_{v_i \in \partial\Omega_H} \tilde{p}_H(v_i) \varphi_i^{(H)}$$

The above sum is taken over vertices v_i on $\partial\Omega_H$. Then, since \tilde{p}_H vanishes on $\partial\bar{\Omega}_H$ it is clear that for the strip formed by the H -elements bordering $\partial\Omega_H$ one has

$$\begin{aligned} h^{-2} \|\tilde{p}_H - p_H\|_0^2 + \|\tilde{p}_H - p_H\|_1^2 &= h^{-2} \|\tilde{p}_H - p_H\|_{0, \text{strip}}^2 + \|\tilde{p}_H - p_H\|_{1, \text{strip}}^2 \\ &\leq CH \sum_{v_i \in \partial\Omega_H} \tilde{p}_H(v_i)^2 \leq C \|\tilde{p}_H\|_{1, \text{strip}}^2 \end{aligned}$$

We then write

$$\mathbf{u}_h = \mathbf{v}_h + \Pi_h^Q(\mathbf{z}_h - \Pi_H^Q \mathbf{z}_H) + \nabla(p_h - \Pi_h^S p_H) + \Pi_h^Q \mathbf{u}_H$$

where $\mathbf{u}_H = \Pi_H^Q \mathbf{z}_H + \nabla p_H$.

Using (16) with (8) gives

$$\|p_h - \Pi_h^S p_H\|_0 \leq Ch \|\nabla p_h\|_0 \leq Ch \|\mathbf{u}_h\|_{\mathbf{H}(\Omega; \text{curl})} \tag{17}$$

We next bound the term $\Pi_h^Q(\mathbf{z}_h - \Pi_H^Q \mathbf{z}_H)$. The problem is that we do not know that Π_h^Q is stable in $L^2(\Omega)$ when applied to such a function. Set \mathbf{C} to be the mean value of \mathbf{z}_h on \hat{K} if $\hat{K} \cap \partial\Omega = \emptyset$, otherwise, set $\mathbf{C} = \mathbf{0}$. As in (7)

$$\|\mathbf{z}_h - \mathbf{C}\|_{0, \hat{K}} \leq Ch \|\mathbf{z}_h\|_{1, \hat{K}}$$

Then

$$\begin{aligned} \|\Pi_h^Q(\mathbf{z}_h - \Pi_H^Q \mathbf{z}_H)\|_{0, K} &= \|\Pi_h^Q(\mathbf{z}_h - \mathbf{C}) + \Pi_h^Q \Pi_H^Q(\mathbf{z}_H - \mathbf{C})\|_{0, K} \\ &\leq C(\|\mathbf{z}_h - \mathbf{C}\|_{0, \hat{K}} + \|\Pi_H^Q(\mathbf{z}_H - \mathbf{C})\|_{0, \hat{K}}) \end{aligned}$$

where we used the triangle inequality, (10) and Theorem 3.1 for the last inequality above. Now, $\mathbf{z}_h - \mathbf{C}$ is a continuous piecewise polynomial on the H -mesh (and vanishes on $\partial\Omega$ when $\hat{K} \cap \partial\Omega \neq \emptyset$) so it follows that

$$\|\Pi_H^Q(\mathbf{z}_H - \mathbf{C})\|_{0, \hat{K}} \leq C \|\mathbf{z}_H - \mathbf{C}\|_{0, \hat{K}} \leq \|\mathbf{z}_H - \mathbf{z}_h\|_{0, \hat{K}} + \|\mathbf{z}_h - \mathbf{C}\|_{0, \hat{K}}$$

Combining the above estimates with limited overlap gives

$$\|\Pi_h^Q(\mathbf{z}_h - \Pi_H^Q \mathbf{z}_h)\|_0 \leq Ch \|\mathbf{z}_h\|_1 \leq Ch \|\mathbf{u}_h\|_{\mathbf{H}(\Omega; \text{curl})}$$

Finally,

$$\|\mathbf{u}_H\|_{\mathbf{H}(\Omega; \text{curl})} \leq CA(\mathbf{u}_h, \mathbf{u}_h)$$

follows from the triangle inequality, (11), (16) and Theorem 5.1.

The theorem follows from (5) and (13) taking \mathbf{u}_H as above and $\mathbf{w}_h = \mathbf{v}_h + \Pi_h^Q(\mathbf{z}_h - \Pi_H^Q \mathbf{z}_H) + \nabla(p_h - \Pi_h^S p_H)$. \square

Remark 5.1

The above proof actually showed that the component \mathbf{u}_H can be chosen as an image of \mathbf{z}_H (under Π_H^Q) from the H^1 -conforming space \mathbf{S}_H plus a gradient of a function in S_H . This fact allows us to derive stable multilevel decompositions based only on conforming finite element functions defined on a hierarchy of meshes \mathcal{T}_{H_k} , $k = 1, 2, \dots, J$. Here the finest auxiliary mesh \mathcal{T}_H corresponds to $H = H_J$. Moreover, the components of the decomposition can be chosen so that they vanish on $\partial\Omega$. Details about such H^1 -conforming multilevel decompositions based on nested spaces are found in Section 6 of [20]. Exploring this fact can lead to a proof of the optimal convergence of the multilevel method using the Hiptmair smoother, resulting from nested Nédélec spaces Q_{H_k} , $k = 1, 2, \dots, J$, supported in Ω . Further details will not be presented here. We only illustrate the performance of such a multilevel method in Section 7.

6. PROOF OF THEOREM 3.1

6.1. Commutativity

Here we consider only lowest order spaces ($r = 0$) S_h , \mathbf{Q}_h , \mathbf{R}_h and their counterparts with indices H . The techniques extend easily to higher order spaces. In what follows, $\boldsymbol{\tau}$ and \mathbf{n} (possibly with subscripts) will denote unit tangential directions along edges and unit normal vectors to faces, respectively, in the tetrahedral meshes.

Since functions in S_H are continuous, the operator Π_h^S is well defined there. The degrees of freedom for Π_h^Q involve integrals of the tangential components along edges of the mesh \mathcal{T}_h . These integrals are obviously well defined for edges which are not tangent to any face of \mathcal{T}_H as functions in \mathbf{Q}_H are piecewise polynomial on such an edge with only point discontinuities. The integrals are well defined along edges when they are tangent to faces of \mathcal{T}_H because the tangential component of a function in \mathbf{Q}_H is continuous there. Similar arguments show that Π_h^R is well defined on \mathbf{R}_H .

Let u be in S_H . To check that $\nabla \Pi_h^S u = \Pi_h^Q \nabla u$ we need only to check that they have the same degrees of freedom since they are both in \mathbf{Q}_h . Consider an edge ℓ in the mesh \mathcal{T}_h with end points v_1 and v_2 and let $\boldsymbol{\tau}_\ell$ be a unit vector pointing from v_1 to v_2 . One has

$$\int_\ell \nabla(\Pi_h^S u) \cdot \boldsymbol{\tau}_\ell \, ds = (\Pi_h^S u)(v_2) - (\Pi_h^S u)(v_1) = u(v_2) - u(v_1)$$

while

$$\begin{aligned} \int_{\ell} \Pi_h^Q(\nabla u) \cdot \boldsymbol{\tau}_{\ell} \, ds &= \int_{\ell} \nabla u \cdot \boldsymbol{\tau}_{\ell} \, ds = \sum_{K_H \cap \ell} \int_{\ell \cap K_H} \nabla u \cdot \boldsymbol{\tau}_{\ell} \, ds \\ &= \sum_{[w_1, w_2] = K_H \cap \ell} (u(w_2) - u(w_1)) = u(v_2) - u(v_1) \end{aligned}$$

We used the fact that u is continuous and that ℓ can be represented as a connected path of line segments $[w_1, w_2] = K_H \cap \ell$.

We check next that $\nabla \times \Pi_h^Q \mathbf{u}$ and $\Pi_h^R(\nabla \times \mathbf{u})$ have the same degrees of freedom (in \mathbf{R}_h) for $\mathbf{u} \in \mathbf{Q}_H$. Stokes' Theorem gives that for any face F of the mesh \mathcal{T}_h

$$\int_F (\nabla \times \Pi_h^Q \mathbf{u}) \cdot \mathbf{n} \, dx = \int_{\partial F} \Pi_h^Q \mathbf{u} \cdot \boldsymbol{\tau} \, ds = \int_{\partial F} \mathbf{u} \cdot \boldsymbol{\tau} \, ds$$

On the other hand, by the definition of Π_h^R , one has

$$\begin{aligned} \int_F (\Pi_h^R(\nabla \times \mathbf{u})) \cdot \mathbf{n} \, ds &= \int_F (\nabla \times \mathbf{u}) \cdot \mathbf{n} \, ds \\ &= \sum_{F \cap K_H} \int_{F \cap K_H} (\nabla \times \mathbf{u}) \cdot \mathbf{n} \, ds \\ &= \sum_{F \cap K_H} \int_{\partial(F \cap K_H)} \mathbf{u} \cdot \boldsymbol{\tau} \, ds \end{aligned}$$

We split the above boundary integrals into integrals along edge segments along the boundary of F and interior segments. Using the fact that $\mathbf{u} \cdot \boldsymbol{\tau}$ is continuous on any interior edge segment, it is clear that each such segment results in two cancelling contributions. Thus

$$\int_F (\Pi_h^R(\nabla \times \mathbf{u})) \cdot \mathbf{n} \, ds = \int_{\partial F} \mathbf{u} \cdot \boldsymbol{\tau} \, ds$$

showing that $\nabla \times \Pi_h^Q \mathbf{u}$ and $\Pi_h^R(\nabla \times \mathbf{u})$ have the same degrees of freedom. This shows the commutativity properties claimed by Theorem 3.1.

6.2. L^2 -stability of Π_h^S , Π_h^Q and Π_h^R on S_H , \mathbf{Q}_H and \mathbf{R}_H

Consider first Π_h^S . Let $\{x_i\}$ and $\{v_i\}$ denote, respectively, the vertices of \mathcal{T}_h and \mathcal{T}_H . Let $T_H(x_i)$ denote a tetrahedron of \mathcal{T}_H containing x_i . For $v_H \in S_H$, by quasi-uniformity

$$\begin{aligned} \|\Pi_h^S v_H\|_0^2 &\leq Ch^3 \sum_{x_i} v_H(x_i)^2 \\ &\leq Ch^3 \sum_{x_i} \sum_{v_j \in T_H(x_i)} v_H(v_j)^2 \leq C \|v_H\|_0^2 \end{aligned}$$

For the last inequality above, we used the fact that there are at most a fixed number (independent of h) of vertices from the h mesh in any element of the H mesh.

Consider next Π_h^Q . Let K be a tetrahedron of \mathcal{T}_h and B_K denote the Jacobian of the affine transformation F_K which maps the reference tetrahedron \bar{K} onto K . The restrictions of functions in Π_h^Q to the element K are mapped to functions in the Nédélec space on the reference element by the transformation

$$\mathbf{v} \rightarrow B_K^t(\mathbf{v} \circ F_K)$$

Moreover the degrees of freedom are mapped according to the formula

$$(\Pi_h^Q \mathbf{v}) \circ F_K = B_K^{-t} \bar{\Pi}^Q(B_K^t(\mathbf{v} \circ F_K))$$

Here $\bar{\Pi}^Q$ denotes the Nédélec interpolation operator on the reference element. The following norm equivalences are a consequence of the equivalence of norms on the reference space and scaling arguments

$$\|\mathbf{u}_h\|_{L_\infty(K)} \simeq \left(\sum_{i=1}^6 (\mathbf{u}_h(\mathbf{v}_i) \cdot \boldsymbol{\tau}_i)^2 \right)^{1/2} \simeq h^{-3/2} \|\mathbf{u}_h\|_{0,K}$$

Here we have used the notation \simeq to denote norm equivalence with constants independent of h . Also, \mathbf{v}_i is the centre of the i th edge e_i of K and $\boldsymbol{\tau}_i$ is the unit vector tangent to e_i .

Given $\mathbf{u}_H \in \mathbf{Q}_H$, one has

$$\|\Pi_h^Q \mathbf{u}_H\|_{0,K}^2 \simeq h^3 \sum_{i=1}^6 \left(\frac{1}{|\ell_i|} \int_{\ell_i} \mathbf{u}_H \cdot \boldsymbol{\tau}_i \, ds \right)^2$$

Moreover,

$$\begin{aligned} \frac{1}{|\ell_i|} \int_{\ell_i} |\mathbf{u}_H \cdot \boldsymbol{\tau}_i| \, ds &= \frac{1}{|\ell_i|} \sum_{\ell_i \cap K_H} \int_{\ell_i \cap K_H} |\mathbf{u}_H \cdot \boldsymbol{\tau}_i| \, ds \\ &\leq \sum_{\ell_i \cap K_H} \|\mathbf{u}_H\|_{L_\infty(K_H)} \end{aligned}$$

Since the number of elements K_H intersecting ℓ_i is bounded, one gets

$$\begin{aligned} \|\Pi_h^Q \mathbf{u}_H\|_{0,K}^2 &\leq Ch^3 \sum_{\ell_i \cap K_H} \|\mathbf{u}_H\|_{L_\infty(K_H)}^2 \\ &\leq Ch^3 \|\mathbf{u}_H\|_{L_\infty(\hat{K})}^2 \\ &\leq C \|\mathbf{u}_H\|_{0,\hat{K}}^2 \end{aligned}$$

The L^2 -stability of Π_h^Q follows by summation. The proof of the L^2 -stability of Π_h^R is similar.

Remark 6.1

The above proofs can be easily extended to other piecewise-polynomial spaces. For example, if \mathbf{V}_H is a discrete space where $\mathbf{\Pi}_h^Q$ is well defined, then there exists $C > 0$ such that

$$\|\mathbf{\Pi}_h^Q \mathbf{u}_H\|_0 \leq C \|\mathbf{u}_H\|_0$$

for any $\mathbf{u}_H \in \mathbf{V}_H$.

7. NUMERICAL EXPERIMENTS

In this section we present numerical results from experiments with different versions of the two-level preconditioner applied to the problem for $\mathbf{u} \in \mathbf{Q}_h$, such that for a given $\mathbf{f} \in \mathbf{L}^2(\Omega)$

$$(\mathbf{u}, \mathbf{v}) + (\nabla \times \mathbf{u}, \nabla \times \mathbf{v}) = (\mathbf{f}, \mathbf{v}) \quad \text{for all } \mathbf{v} \in \mathbf{Q}_h$$

Specifically, we considered

1. The multiplicative version of the preconditioner (2) with B_H being a $V(1, 1)$ cycle of geometric multigrid (with Hiptmair smoothing) on the auxiliary mesh.
2. The additive preconditioner (2) with geometric multigrid on the auxiliary mesh.
3. The multiplicative preconditioner with exact solve on the auxiliary mesh.
4. The additive preconditioner with exact solve on the auxiliary mesh (\tilde{B}_h).

In all experiments we used the lowest order Nédélec space for computing the entries of A_h and F , with a right-hand side $\mathbf{1}$ and homogeneous boundary conditions. We also employed the multiplicative version of the Hiptmair smoother. The auxiliary mesh was chosen to be uniform, for the efficiency reasons addressed in Section 8.2.

We first present results in two dimensions (see Section 8.1 for details). We chose two initial meshes on the unit square and used uniform refinement to generate larger problems, as shown in Figure 2. The refinement levels were synchronized such that the mesh size ratio is kept at approximately 1.06.

Results of the preconditioned conjugate gradient iteration using the two-level preconditioners are reported in Table I. The iterations were stopped after the norm of the initial residual was reduced by six orders of magnitude. The empty spots indicate that the execution time was too

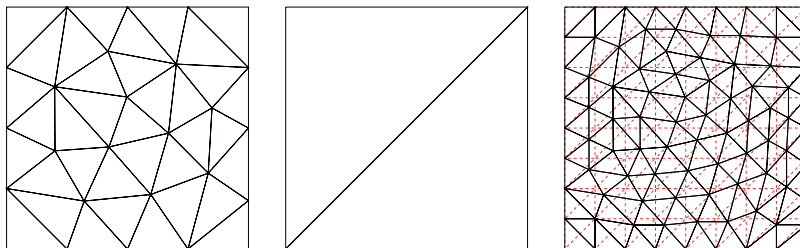


Figure 2. Initial mesh on the unit square (left), initial auxiliary mesh (centre) and the composition of the two meshes after refinement (right).

Table I. Numerical results for the problem on the unit square.

ℓ	N	ℓ_{aux}	N_{aux}	n_1	n_2	n_3	n_4
0	62	2	56	4	8	3	8
1	232	3	208	4	9	4	9
2	896	4	800	4	9	4	9
3	3520	5	3136	4	9	3	8
4	13 952	6	12 416	4	8	3	8
5	55 552	7	49 408	4	8	3	7
6	221 696	8	197 120	4	7	3	7
7	885 760	9	787 456	4	7		
8	3 540 992	10	3 147 776	4	7		

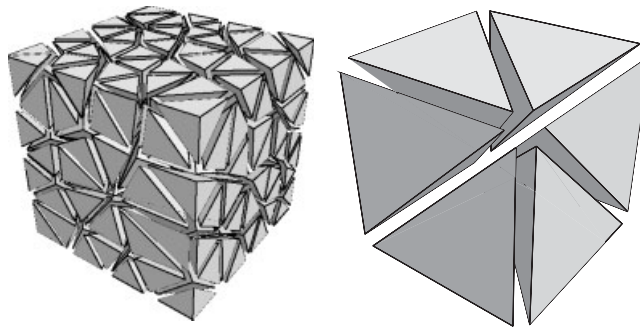


Figure 3. Initial mesh on the unit cube (left) and initial auxiliary mesh (right).

long. We use the following notation: ℓ is the refinement level of \mathcal{T}_h , N is the size of the problem in \mathbf{Q}_h . The same quantities for the auxiliary mesh are denoted with ℓ_{aux} and N_{aux} . In the last four columns we report the iteration count for each of the two-level preconditioners (1)–(4).

The results in Table I confirm that both the multiplicative and the additive versions lead to solution methods with bounded number of iterations. The additive preconditioner requires approximately twice as many iterations (but it is cheaper to compute). Another interesting observation is that using multigrid instead of exact solver on the auxiliary mesh, in both cases, leads to almost no increase in the number of iterations.

Next, we repeat the same experiment on an unstructured mesh on the unit cube, shown in Figure 3. As before, we refine both meshes, keeping the mesh size ratio at approximately 1.07.

The behaviour of the two-level preconditioners is presented in Table II and is similar to the two-dimensional case.

Again, we have a bounded number of iterations with the additive count being approximately twice larger. As in Table I, using multigrid instead of exact solve increases the number of iterations, at most, by one.

In the next set of examples, we allow for the auxiliary mesh to be defined on a domain Ω_H , that differs from the original domain Ω . This situation is of practical interest, since it allows for a problem defined on a very complicated mesh to be preconditioned by geometric multigrid on a

Table II. Numerical results for the problem on the unit cube.

ℓ	N	ℓ_{aux}	N_{aux}	n_1	n_2	n_3	n_4
0	722	2	604	4	9	4	9
1	5074	3	4184	5	10	4	10
2	37 940	4	31 024	6	16	5	16
3	293 224	5	238 688	6	16	6	15
4	2 305 232	6	1 872 064	6	16		

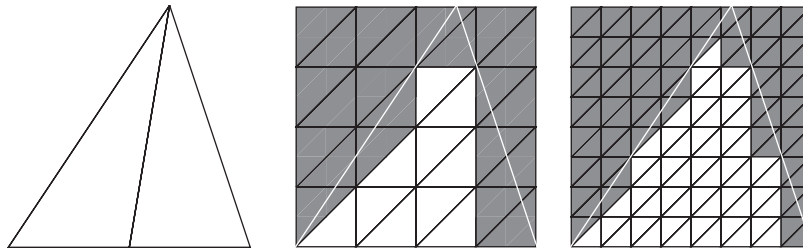


Figure 4. Initial mesh on the triangular domain and two auxiliary meshes inscribed in it.

Table III. Numerical results for the problem on the triangular domain.

ℓ	N	ℓ_{aux}	N_{aux}	n_1	n_2	n_3	n_4
4	800	4	800	10	17	8	16
5	3136	5	3136	11	19	8	16
6	12 416	6	12 416	12	20	8	16
7	49 408	7	49 408	12	20	7	15
8	197 120	8	197 120	13	20	7	14
9	787 456	9	787 456	13	20		
10	3 147 776	10	3 147 776	13	20		

box. Similar approaches for second order elliptic problems have been known as ‘fictitious’ domain or domain embedding methods and can lead to optimal multigrid preconditioners, see [2].

To demonstrate the algorithm, we set to precondition our discrete problem posed on a simple triangular domain by using the uniform auxiliary mesh from our first experiment. On each refinement level, we define Ω_H by removing all elements of the auxiliary mesh that are not inside Ω . The process is illustrated in Figure 4. Since $\Omega_H \subset \Omega$, we get a sequence of nested auxiliary subspaces of $\mathbf{H}_0(\Omega; \text{curl})$, for which we define our geometric multigrid preconditioner (based on Hiptmair smoothing). One simple way to implement this in practice is to eliminate all degrees of freedom corresponding to the removed elements from the stiffness matrices and all interpolation and smoothing operators.

The results for the so-defined non-matching auxiliary mesh preconditioner are listed in Table III. One observes that the number of iterations is larger than in the previous 2D experiment, but it eventually stabilizes. Compared to the earlier results, the gap between the two-level and the multigrid methods is larger.

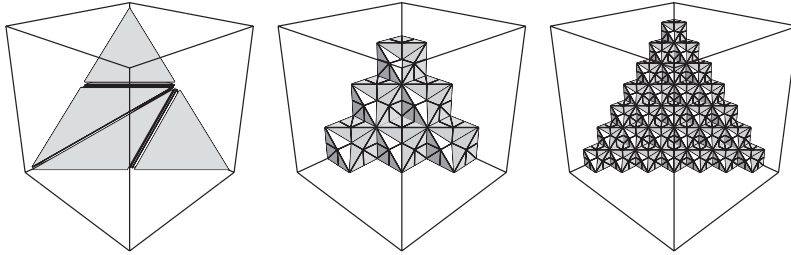


Figure 5. Initial mesh on the tetrahedral domain and two auxiliary meshes inscribed in it.

Table IV. Numerical results for the problem on the reference tetrahedron.

ℓ	N	ℓ_{aux}	N_{aux}	n_1	n_2	n_3	n_4
2	804	2	604	10	20	10	20
3	5576	3	4184	14	33	13	32
4	41 360	4	31 024	16	40	14	37
5	318 240	5	238 688	18	45	14	40
6	2 496 064	6	1 872 064	19	46		

Our last test is a non-matching auxiliary mesh example in 3D where Ω is the reference tetrahedron, with vertices $(0, 0, 0)$, $(1, 0, 0)$, $(0, 1, 0)$ and $(0, 0, 1)$, split into eight elements. We used the uniform auxiliary mesh from the second example. The two meshes were refined such that the mesh size ratio on each level is approximately 1.10. The initial mesh and two auxiliary meshes Ω_H are shown in Figure 5.

The numerical results in Table IV suggest that, as with the previous test, the non-matching auxiliary mesh preconditioner requires more iterations and more refinement levels to exhibit its asymptotic behaviour. In this case, the multiplicative methods performed significantly better than the additive ones. Finally, while the two-level methods seem to be optimal, the number of iterations for the first two preconditioners are slightly increasing.

8. CONCLUDING REMARKS

8.1. Two-dimensional problems

Even though we concentrated on the 3D case, the theory of the preceding sections can be modified such that the results hold for two-dimensional problems. Below we outline how this can be done.

Assume that Ω is a convex polygonal domain discretized with a triangular mesh. One defines $\mathbf{H}(\Omega; \text{curl})$ as

$$\mathbf{H}(\Omega; \text{curl}) = \{\mathbf{u}^\perp : \mathbf{u} \in \mathbf{H}(\Omega; \text{div})\}$$

where $\mathbf{u}^\perp = (-u_2, u_1)$ is the $\pi/2$ rotation of the vector field $\mathbf{u} = (u_1, u_2)$. Furthermore, $\nabla \times \mathbf{u}^\perp$ is defined to be $\nabla \cdot \mathbf{u}$, and the Nédélec space \mathbf{Q}_h keeps its definition provided we consider $\mathbf{x} \in \mathbb{R}^2$. The properties of the Hiptmair smoother are well known in 2D. The stable decomposition (14)

also holds in this case, see [7]. Thus, the proof of Theorem 5.2 needs no changes, as long as the estimate

$$\|\nabla \times \mathbf{\Pi}_h^Q \mathbf{u}\|_0 \leq C \|\nabla \times \mathbf{u}\|_0 \tag{18}$$

from Corollary 3.1 is available.

Since the right half of the commuting diagram (6) is defined only in 3D, we prove the above estimate directly. Fix $K \in \mathcal{T}_h$ and $\mathbf{u} \in \mathbf{Q}_H$. Then

$$\int_K \nabla \times \mathbf{\Pi}_h^Q \mathbf{u} \, dx = \int_{\partial K} \mathbf{\Pi}_h^Q \mathbf{u} \cdot \boldsymbol{\tau} \, ds = \int_{\partial K} \mathbf{u} \cdot \boldsymbol{\tau} \, ds = \int_K \nabla \times \mathbf{u} \, dx$$

For the lowest order Nédélec space, $\nabla \times \mathbf{\Pi}_h^Q \mathbf{u}$ is a constant in K , so

$$\|\nabla \times \mathbf{\Pi}_h^Q \mathbf{u}\|_{0,K}^2 = \frac{1}{\mu(K)} \left(\int_K \nabla \times \mathbf{u} \, dx \right)^2 \leq \|\nabla \times \mathbf{u}\|_{0,K}^2$$

where $\mu(K)$ is the measure of K . This completes the proof of (18), and therefore we can conclude that our main results hold in two dimensions.

8.2. Efficient implementation of $\mathbf{\Pi}_h^Q$

The only non-standard part of the solution algorithm is the computation of the matrix representation of $\mathbf{\Pi}_h^Q$. This requires that for every basis function $\boldsymbol{\phi}$ of \mathbf{Q}_H one evaluates and stores the integrals $\int_{\ell} \boldsymbol{\phi} \cdot \boldsymbol{\tau}_i \, ds$ over all edges ℓ of \mathcal{T}_h . In order to keep optimal complexity, this has to be done only for the integrals that are not zero, i.e. only for edges ℓ belonging to elements in \mathcal{T}_h which intersect the support of $\boldsymbol{\phi}$. Thus, an efficient implementation requires that we have a relation table, **AuxElement_Element**, which for each (auxiliary) element in \mathcal{T}_H gives the list of elements in \mathcal{T}_h that intersect it. In practice, it might be easier to construct the above relation table (implemented as a boolean sparse matrix, for example) as the transpose of the similar **Element_AuxElement**. In particular, if the auxiliary mesh is uniform, one can directly enumerate all auxiliary elements intersecting, e.g. the bounding box of a given element in \mathcal{T}_h , since the auxiliary vertices form a simple lattice. If the auxiliary mesh is not uniform, the computation of **AuxElement_Element** becomes much more involved, and should probably be incorporated in the mesh generation process, in order to achieve optimal complexity.

REFERENCES

1. Bramble JH, Pasciak JE, Zhang X. Two-level preconditioners for 2m'th order elliptic finite element problems. *East-West Journal of Numerical Mathematics* 1996; **4**:99–120.
2. Xu J. The auxiliary space method and optimal preconditioning techniques for unstructured grids. *Computing* 1996; **56**:215–235.
3. Brenner SC. Preconditioning complicated finite elements by simple finite elements. *SIAM Journal on Scientific Computing* 1996; **17**(5):1269–1274.
4. Buzbee BL, Dorr FW, George JA, Golub GH. The direct solution of the discrete Poisson equation on irregular regions. *SIAM Journal on Numerical Analysis* 1971; **8**:722–736.
5. Astrakhansev GP. Method for fictitious domains for a second-order elliptic equation with natural boundary conditions. *U.S.S.R. Computational Mathematics and Mathematical Physics* 1978; **18**:114–121.
6. Hiptmair R, Widmer G, Zou J. Auxiliary space preconditioning in $H(\text{curl})$. *Numerische Mathematik* 2006; **103**(3):435–459.

H(CURL) AUXILIARY MESH PRECONDITIONING

7. Hiptmair R, Xu J. Nodal auxiliary space preconditioning in $H(\text{curl})$ and $H(\text{div})$ spaces. *Technical Report 2006-09*, ETH, Switzerland, 2006.
8. Kolev TzV, Vassilevski PS. Some experience with a H^1 -based auxiliary space AMG for $H(\text{curl})$ problems. *Technical Report UCRL-TR-221841*, LLNL, June 2006.
9. Kolev TzV, Vassilevski PS. Parallel H^1 -based auxiliary space AMG solver for $H(\text{curl})$ problems. *Technical Report UCRL-TR-222763*, LLNL, July 2006.
10. Hiptmair R. Finite elements in computational electromagnetism. *Acta Numerica* 2002; **11**:237–339.
11. Hiptmair R. Multigrid method for Maxwell's equations. *SIAM Journal on Numerical Analysis* 1999; **36**(1): 204–225.
12. Arnold DN, Falk RS, Winther R. Multigrid in $\mathbf{H}(\text{div})$ and $\mathbf{H}(\text{curl})$. *Numerische Mathematik* 2000; **85**:197–217.
13. Hiptmair R, Toselli A. Overlapping Schwarz methods for vector valued elliptic problems in three dimensions. *Parallel Solution of PDEs*, IMA Volumes in Mathematics and its Applications. Springer: Berlin, 1998.
14. Smith BF, Bjørstad PE, Gropp WD. *Domain Decomposition. Parallel Multilevel Methods for Elliptic Partial Differential Equations*. Cambridge University Press: Cambridge, 1996.
15. Brezzi F, Fortin M. *Mixed and Hybrid Finite Element Methods*. Springer: New York, 1991.
16. Girault V, Raviart PA. *Finite Element Approximation of the Navier–Stokes Equations*. Lecture Notes in Mathematics, vol. 749. Springer: New York, 1981.
17. Amrouche C, Bernardi C, Dauge M, Girault V. Vector potentials in three-dimensional non-smooth domains. *Mathematical Methods in the Applied Sciences* 1998; **21**(9):823–864.
18. Brenner SC, Scott LR. *The Mathematical Theory of Finite Element Methods*. Springer: New York, 1994.
19. Pasciak JE, Zhao J. Overlapping Schwarz methods in $\mathbf{H}(\text{curl})$ on polyhedral domains. *Journal of Numerical Mathematics* 2002; **10**:221–234.
20. Bramble JH. *Multigrid Methods*. Pitman Research Notes in Mathematics Series, vol. 294. Longman Scientific & Technical: Harlow, U.K., 1993.